

***discordia* mutations specifically misorient asymmetric cell divisions during development of the maize leaf epidermis**

Kimberly Gallagher and Laurie G. Smith*

Department of Biology, University of California at San Diego, 9500 Gilman Drive, La Jolla, CA 92093-0116, USA

*Author for correspondence (e-mail: lsmith@biomail.ucsd.edu)

Accepted 29 July; published on WWW 27 September 1999

SUMMARY

In plant cells, cytokinesis depends on a cytoskeletal structure called a phragmoplast, which directs the formation of a new cell wall between daughter nuclei after mitosis. The orientation of cell division depends on guidance of the phragmoplast during cytokinesis to a cortical site marked throughout prophase by another cytoskeletal structure called a preprophase band. Asymmetrically dividing cells become polarized and form asymmetric preprophase bands prior to mitosis; phragmoplasts are subsequently guided to these asymmetric cortical sites to form daughter cells of different shapes and/or sizes. Here we describe two new recessive mutations, *discordial1* (*dcd1*) and *discordial2* (*dcd2*), which disrupt the spatial regulation of cytokinesis during asymmetric cell divisions. Both mutations disrupt four classes of asymmetric cell divisions during the development of the maize leaf epidermis, without affecting the symmetric divisions through which most epidermal cells

arise. The effects of *dcd* mutations on asymmetric cell division can be mimicked by cytochalasin D treatment, and divisions affected by *dcd1* are hypersensitive to the effects of cytochalasin D. Analysis of actin and microtubule organization in these mutants showed no effect of either mutation on cell polarity, or on formation and localization of preprophase bands and spindles. In mutant cells, phragmoplasts in asymmetrically dividing cells are structurally normal and are initiated in the correct location, but often fail to move to the position formerly occupied by the preprophase band. We propose that *dcd* mutations disrupt an actin-dependent process necessary for the guidance of phragmoplasts during cytokinesis in asymmetrically dividing cells.

Key words: Asymmetric cell division, Cytokinesis, Maize, Leaf development, Actin, *discordial1* (*dcd1*)

INTRODUCTION

A fundamental question in the development of all multicellular organisms is how, from one cell, the cellular diversity of the organism is achieved. Asymmetric cell division is one of the mechanisms contributing to this diversity and is therefore important for normal development. Broadly speaking, an asymmetric division is one that gives rise to daughter cells with different fates (Horvitz and Herskowitz, 1992). In some well studied cases in animals and yeast, proper specification of daughter cell fates is known to depend on polarization of the mother cell and precise orientation of an asymmetric division plane to segregate cell fate determinants unequally between the daughters (e.g., Rhyu and Knoblich, 1995; Tazikawa et al., 1997). Plant development offers many examples of cell divisions that are not only developmentally asymmetric but also physically asymmetric in that they produce daughter cells of different shapes or sizes (Gallagher and Smith, 1997). In plants, specialized cells performing a variety of tissue functions are organized into complexes that often arise through asymmetric cell divisions. In order for the cells in these complexes to work together, they must have appropriate shapes and sizes, and be correctly positioned relative to each other.

Since the shapes, sizes and tissue locations of plant cells are defined by their walls, formation of such complexes depends on control of wall placement during cytokinesis. In addition, segregation of cell fate determinants may depend on properly oriented asymmetric cell divisions, as it does in animals and yeast (Eady et al., 1995; Twell et al., 1998).

In animal cells, the orientation of division is determined by the position of the spindle. Cytokinesis, achieved via contraction of the plasma membrane, always occurs in a plane perpendicular to the spindle axis (Rappaport, 1986; Salmon, 1989). In plant cells, the plane of cell division is determined by the position of an actin- and microtubule-containing structure called a phragmoplast, which directs Golgi-derived vesicles containing cell wall materials to a region between the daughter nuclei where they fuse to form a new cell wall (Gunning, 1982; Staehelin and Hepler, 1996). The location of the phragmoplast and new cell wall is predicted during prophase by the position of a transient cortical array of microtubules and actin filaments called the preprophase band (PPB) (Pickett-Heaps and Northcote, 1966; Palevitz, 1987; Traas et al., 1987; Wick, 1991). Though the function of the PPB is not known, it has been proposed that it may mark the division site in a way that allows the phragmoplast to be guided

to this site during cytokinesis (Mineyuki and Gunning, 1990). Indeed, a variety of experiments have shown that the phragmoplast is actively guided during cytokinesis to the site formerly occupied by the PPB (Ota, 1961; Palevitz, 1980; Gunning and Wick, 1985; Cleary and Smith, 1998).

The mechanisms governing phragmoplast guidance to established cortical division sites are unknown. However, it has long been known that cytochalasins, which disrupt the actin cytoskeleton, can misorient new cell walls (Palevitz and Hepler, 1974; Palevitz, 1980; Mineyuki and Palevitz, 1990; Cho and Wick, 1990). This raises the question of how actin participates in the spatial control of cytokinesis. Throughout cell division, actin surrounds the nucleus and actin-containing cytoplasmic strands radiate from the nucleus to the cell cortex (Kakimoto and Shibaoka, 1987; Seagull et al., 1987; Traas et al., 1987). In some cells, actin-containing cytoplasmic strands have been seen to link the edges of the phragmoplast to the cortical division site (Kakimoto and Shibaoka, 1987; Lloyd and Traas, 1988; Valster and Hepler, 1997). Thus, actin-based attachments between the phragmoplast and cell cortex may help guide the phragmoplast to the established division site. All features of F-actin organization during plant cell division mentioned above are also found in asymmetrically dividing cells (Cho and Wick, 1990; Cleary, 1995; Cleary and Mathesius, 1996). Additional observations suggest that actin may play an even greater role in the spatial regulation of asymmetric cell divisions. For example, an early step in the asymmetric division of subsidiary mother cells during stomatal complex formation in *Tradescantia* leaves is the polarization of the mother cell, involving an actin-dependent migration of the nucleus during G₁ to a defined cortical site (Kennard and Cleary, 1997) and subsequent formation of a dense actin patch at this site (Cleary, 1995; Cleary and Mathesius, 1996). Following entry into mitosis, the spindle and phragmoplast remain closely associated with the cortical actin patch; treatment with cytochalasin causes dissociation of the nucleus from the actin patch and ultimately, mis-localization of the new cell wall (Pickett-Heaps et al., 1999).

The maize leaf is an excellent system for studying asymmetric cell divisions during plant development. Most of the cells making up the leaf arise through proliferative divisions, which are symmetric and oriented either transversely or longitudinally (Sharman, 1942; Sylvester et al., 1990). Asymmetric divisions are involved in the formation of specialized cell types, and mostly occur after proliferative divisions have been completed (Sylvester et al., 1996). In the maize leaf epidermis, asymmetric divisions are involved in the formation of both stomatal complexes and silica-cork cell pairs. In this study, we report the isolation and analysis of two new, recessive mutants, *discordial* (*dcd1*) and *discordia2* (*dcd2*), in which these asymmetric cell divisions are specifically misoriented. Analysis of these mutants presented here suggests that they disrupt an actin-dependent process involved in the spatial regulation of asymmetric cell divisions.

MATERIALS AND METHODS

TBO staining of epidermal peels

Adult leaves (defined here as leaves number 8-12, counting the first leaf to be initiated as leaf number 1) from nine plants of each genotype

(wild-type, *dcd1* and *dcd2*) were cut into 1 cm squares and fixed in 4% formaldehyde in 50 mM KPO₄, 5.0 mM EDTA and 0.2% saponin pH 7 for at least 2 hours at room temperature (RT). Tissue pieces were then washed 2-5 times in dH₂O, digested in 0.1% pectolyase (Sigma, St. Louis) in dH₂O for at least 2 hours at RT then rinsed in dH₂O. The epidermis was then peeled from the rest of the leaf and incubated in 0.05% TBO pH 4.0 until evenly stained. Peels were mounted in water and photographed under bright-field conditions on a Nikon Eclipse E600 microscope using a 10× objective on Kodak Ektachrome 160T slide film or Royal Gold 100 print film.

Analysis of cell division

To examine cell walls and nuclei in regions of the leaf where cells are dividing, immature leaves were stained with acriflavin orange (Sigma, St. Louis) as described by Cleary and Smith (1998). For this analysis, tissue pieces were taken from the basal 4 cm of immature adult leaves (leaf numbers 8-12 when 4-12 cm long) from 10 wild-type and 10 mutant plants. Following acriflavin staining, leaf samples were viewed on a Zeiss laser scanning confocal microscope with a 40× 1.4 NA oil-immersion objective as described by Cleary and Smith (1998). All acriflavin images shown are single mid-plane optical sections.

Cytochalasin treatments

To examine the effects of cytochalasin D (CD) on cell division, strips of leaf tissue 3-10 mm wide by 1-2 cm long were removed aseptically from the basal 4 cm of immature, adult leaves (as defined above) and placed into tissue culture. Culture medium consisted of 1× MS salts (Gibco-BBL, Grand Island) with 0.06 M sucrose and 0.2 M sorbitol pH 5.8 (basal medium). 2.0 ml of basal medium containing 1.5% agarose was dispensed into 12-well plates (Costar, Nagog Park). After this had solidified, an overlayer was added consisting of 200 µl of basal medium containing 0.3% agarose with DMSO and/or CD at concentrations which, after diffusion, would result in a final concentration of 0.5% DMSO alone or with 1.0, 5.0 or 10.0 µM CD in the 2.2 ml culture. After 2-4 hours in the dark, to allow for diffusion of DMSO and/or CD, tissues were laid flat on the media and incubated at 23°C in a 16-hour light/8-hour dark cycle for 48 hours. Following incubation all sample were processed for acriflavin staining and visualized as described above. All concentrations of CD were tested at least twice with a minimum of 4 different plants represented in each trial. In total, >2000 subsidiary cells were analyzed to produce the data shown in Fig. 7. In order to include in our analysis only those subsidiary cell divisions that had occurred in culture, we counted stomata in which the guard cells had not yet formed (this is most of the sample) or had recently divided, as judged by the state of other GMCs in the file or (in >5.0 µM CD) the orientation of the guard cell walls. Regardless of the above criteria, any samples having fully developed bulliform rows or prickle hairs were excluded from the analysis. When very immature tissue was put into culture at a stage prior to most GMC and all subsidiary cell formation, stomata lacking subsidiaries were often observed even in the absence of DMSO. We considered this as an artifact of tissue culture and not a result of DMSO or CD treatment. Such stomata were not counted in our analysis of subsidiary cell divisions, but were considered in our analysis of GMC formation.

Analysis of the cytoskeleton

The basal 4 cm of immature adult leaves (as defined above) were removed, cut into 1-3 mm strips of varying lengths and processed for either visualization of microtubules or actin as described by Cleary and Smith (1998) with the following modifications. To visualize subsidiary formation the tissues were digested with a lower concentration of cell wall digesting enzymes (1% driselase and 0.5% pectolyase) for 25-30 minutes. In all experiments, antibody incubations (both primary and secondary) were performed under a weak vacuum for the first 2 hours. Fluorescence was visualized on either a Zeiss laser scanning confocal microscope with a 1.4 NA 63×

oil-immersion lens or a Nikon Optiphot microscope equipped with a Biorad laser scanning confocal system with a 1.4 NA 60× oil-immersion lens using filter sets recommended for visualizing FITC or propidium iodide (PI). In some cases, multiple optical sections were collected from a single field and flattened into a projection using image processing software provided by Zeiss or BioRad. Red-green images shown in Figs 8 and 9 were produced using the Zeiss or Biorad image processing software or Adobe Photoshop 4.0.1. Measurements of the distance from the SMC phragmoplast to the GMC were made using either Canvas version 3.5 or 5.0 caliper tool with x.xx inch precision. The measurements were converted to pixels and then to microns. Data presented in the text and in Fig. 8 represent a total of 75 wild-type, 82 *dcd1* and 73 *dcd2* phragmoplasts examined in leaf samples from greater than 10 plants of each genotype. In these samples the position of >250 microtubule PPBs and the corresponding nuclei were also examined.

RESULTS

dcd1 and *dcd2* were isolated in a screen for new, EMS-induced mutations affecting epidermal cell pattern in maize. Both mutations affect cell pattern on the abaxial and adaxial surfaces of juvenile and adult leaves, and segregate as single gene, recessive traits in the B73 background. Complementation tests showed that these mutations are non-allelic, and thus define different genes. *dcd1* has been mapped using B-A translocations (Beckett, 1994) to the long arm of chromosome 10. The chromosome arm location of *dcd2* has not yet been determined.

Effects of *discordia* mutations on epidermal cell pattern

To investigate how *dcd1* and *dcd2* affect cell pattern, epidermal peels were stained with toluidine blue O (TBO). As seen in Fig. 1A, stomatal complexes in wild-type leaves are composed of very narrow guard cell pairs, which stain dark purple with TBO, flanked by lens-shaped subsidiary cells, which stain pink or light purple, and are contained within the boundaries of the file from which the associated guard cells originated (Fig. 1A, arrows). In *dcd1* and *dcd2* mutant leaves, stomatal subsidiary cells are often misshapen and extend beyond the file from which the associated guard cells originated (Fig. 1B-D, arrows).

Examination of TBO-stained epidermal peels showed that *dcd1* and *dcd2* mutations also affect formation of silica and cork cell pairs. As illustrated in Fig. 1E, silica and cork cells are formed in pairs; silica cells are smaller and stain pink with TBO whereas cork cells are larger and stain blue. Silica and cork cell pairs are found mainly within non-specialized epidermal cell files (Fig. 1A, arrowheads). In *dcd1* and *dcd2* mutants, the silica and cork cells are not always the correct size or shape and do not always show differential staining (Figs 1B,C,F,G, arrowheads). There are also occasional duplications of silica and cork cells such that they are clustered into groups of four or more cells (Fig. 1G). The frequency of abnormal silica and cork cells is highly variable and does not correlate either directly or inversely with the frequency of abnormal subsidiary cells. This is illustrated in Fig. 1C and D, which show two different *dcd2* mutant leaves. The frequency of abnormal subsidiary cells in these leaves is the same, but in C there is also a high frequency of abnormal silica and cork cells,

which is not seen in D. The abnormal shapes of subsidiary, silica and cork cells often distort the regularity of the surrounding cell files, but other epidermal cell types do not appear to be directly affected by these mutations. In addition, examination of transverse sections of *dcd1* leaves gave no indication of abnormal cell pattern in the internal tissue layers of the leaf (data not shown).

Effects of *discordia* mutations on epidermal cell divisions

The abnormalities we observed in stomatal subsidiaries and silica-cork cell pairs suggested that the specialized cell divisions that form these cell types are perturbed in some way. To further investigate this, developing leaves were fixed at stages when these divisions occur and stained with acriflavin orange to fluorescently label cell walls and nuclei. The stained leaves were then examined with confocal microscopy.

Stomatal divisions

As previously described in maize and other grasses (Stebbins and Shah, 1960; Giles and Shehata, 1984) and illustrated in Fig. 2A, the formation of wild-type stomatal complexes begins with an asymmetric, transverse division of a cell we refer to as a guard cell progenitor (GCP); it divides to produce an apical guard mother cell (GMC, arrowheads in Fig. 2A) and a basal interstomatal cell. GMCs subsequently elongate (Fig. 2B, arrowheads) and prior to formation of the guard cells, subsidiary cells are formed from subsidiary mother cells (SMCs) located immediately adjacent to the GMC. Premitotic nuclei in the SMCs migrate to the longitudinal walls adjacent to the GMC (Fig. 2C, arrows). Subsequently these nuclei divide and a new wall is laid down around the inner nucleus to form a subsidiary cell (Fig. 2C, arrows). By this time, GMCs are narrower than the cells above and below, and subsidiary cell walls are formed within the boundaries of the GMC-containing file. Following subsidiary cell formation, each GMC divides longitudinally to produce two guard cells (not shown).

As expected from our observations on the effects of *discordia* mutations on epidermal cell pattern, we found that these mutations alter the asymmetric divisions involved in subsidiary cell formation. In *dcd1* and *dcd2*, nuclear alignment occurs properly, followed by nuclear division and formation of the subsidiary cell wall. As illustrated in Fig. 2D and E, however, subsidiary cell walls are often mispositioned. The frequency of abnormal subsidiary divisions in *dcd1* mutants is 30±9% ($n>450$) and 52±12% ($n>100$) in *dcd2*. In some *dcd2* leaves, the frequency of abnormal subsidiary cell divisions approaches 100%. To determine whether there is any polarity or regularity to the aberrant subsidiary divisions, we arbitrarily assigned numbers to the SMC walls and analyzed the abnormal attachment points of the newly formed subsidiary cell walls with reference to these numbers (Fig. 3A). As shown in Figs 2D,E, 3, one end of the subsidiary cell wall is usually attached at a correct position near the GMC. There is no propensity for this normal attachment to be either at the apical or the basal GMC wall. The abnormally attached end can be connected to either the transverse (1) or longitudinal (2 or 3) walls of the SMC. As illustrated in Fig. 3B, abnormal attachments are most frequently made to the short, transverse wall (no. 1) in both mutants and to cell corners in *dcd2*, and least frequently to wall

3, the longitudinal wall adjacent to the GMC. These data suggest a tendency of new cell walls in abnormally dividing cells to remain straight rather than curving around the inner daughter nucleus. Occasionally, one end of the new cell wall fails to make any attachment with the SMC wall and instead loops back on itself forming a structure resembling a lariat (Fig. 3B, arrow O). Interestingly, when the subsidiary cell division is aberrant, it sometimes appears that a second division takes place, often producing a normal subsidiary cell (Figs 2D and 3C, arrows). This phenomenon was also described in an earlier study in which subsidiary divisions in maize were misoriented by centrifugation (Galatis et al., 1984).

Although not expected from our observations of mature, TBO-stained epidermal peels, we noted that *dcd* mutations also affect the asymmetric, transverse divisions that form GMCs. In preparation for this division, nuclear migration to the apical end of the GCP occurs as in wild-type. However, the new cell wall formed is often oblique, curved or nearly longitudinal (Fig. 4B,C). Similar to the abnormal subsidiary cell divisions, one end of the GMC wall is usually attached correctly; the other end may be attached to any of the GCP walls. The frequency of aberrant GMCs in *dcd1* is highly variable. Some *dcd1* mutant leaves we examined had no indication of abnormal GMC-forming divisions ($n > 200$), but in others, the frequency of abnormal GMC-forming divisions in a single stomatal file was as high as 19%. This aspect of the phenotype appears to be more penetrant in *dcd2* mutants, where the average frequency of abnormal GMC-

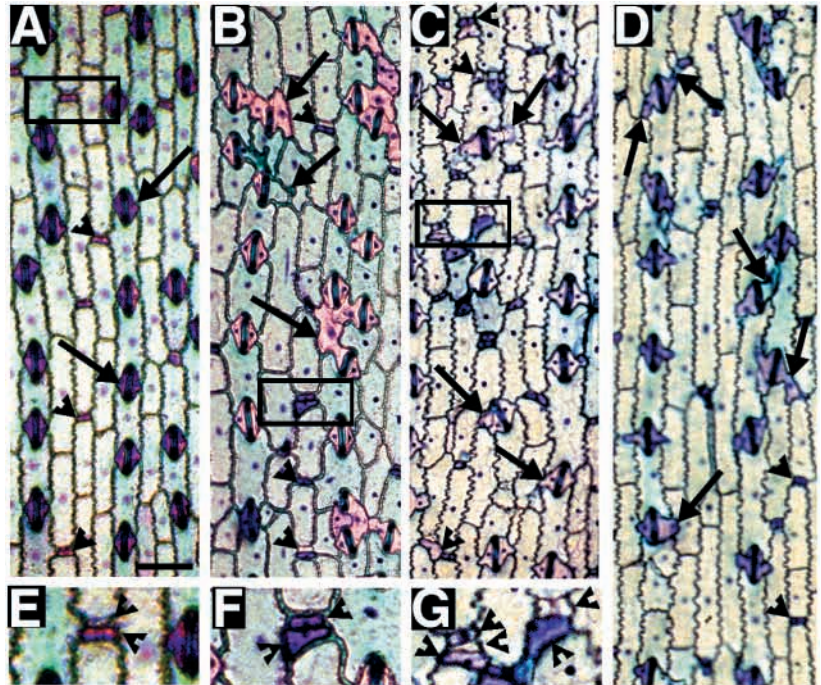
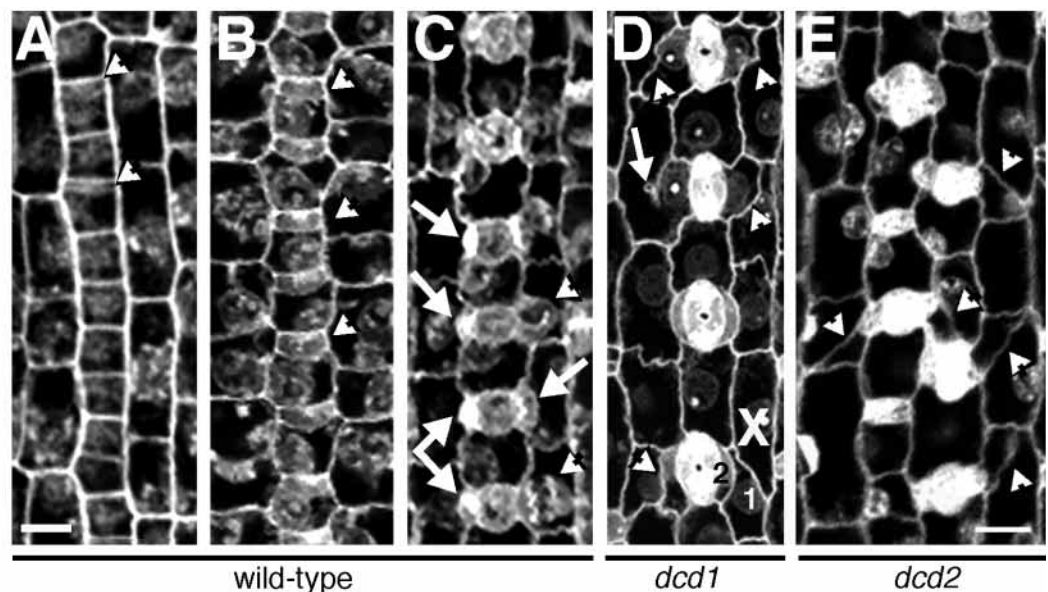


Fig. 1. Effects of *dcd* mutations on cell pattern in the maize leaf epidermis, as seen in TBO-stained epidermal peels. (A) Wild-type epidermis with normal files of stomata (arrows) and silica-cork cell pairs (arrowheads). (B) *dcd1* epidermis with abnormal stomata (arrows), and both normal and abnormal silica and cork cells (arrowheads). (C) *dcd2* epidermis with mildly affected subsidiary cells (arrows) and profoundly affected silica and cork cell pairs (arrowheads). (D) *dcd2* epidermis with moderately affected subsidiary cells (arrows) but normal silica-cork cell pairs (arrowheads). (E) Boxed area of wild-type epidermis shown in A at higher magnification. Arrowheads point to silica (upper cell) and cork (lower cell) pair. (F) Boxed area of *dcd1* epidermis shown in B at higher magnification. Arrowheads point to abnormal cells of silica and cork cell pair. (G) Boxed area of *dcd2* epidermis shown in C at higher magnification. Arrowheads point to abnormal cells of silica and cork cell cluster. Scale bar, 100 μ m.

Fig. 2. Subsidiary cell divisions in wild-type and *dcd* mutant leaves. (A) Wild-type: a file of square GCPs is shown. GCPs divide transversely and asymmetrically to produce GMCs (arrowheads). (B) Wild-type: GMCs elongate (arrowhead). (C) Wild-type: SMC nuclei migrate to the GMC wall (arrowheads) and subsidiary cells have formed in many of the SMCs (arrows). (D) *dcd1* epidermis at a stage later than that shown in C. Note the recent, abnormal subsidiary cell divisions (arrowheads). Note in SMC marked with 'X' a normal subsidiary cell '2' has apparently formed after an abnormal subsidiary cell indicated by a '1'. Arrow points to an incomplete wall in this SMC. (E) *dcd2* epidermis at a stage similar to that shown in C also with many aberrantly oriented subsidiary cell walls (arrowheads). A-D are same magnification. Scale bars, 17.0 μ m.



(E) *dcd2* epidermis at a stage similar to that shown in C also with many aberrantly oriented subsidiary cell walls (arrowheads). A-D are same magnification. Scale bars, 17.0 μ m.

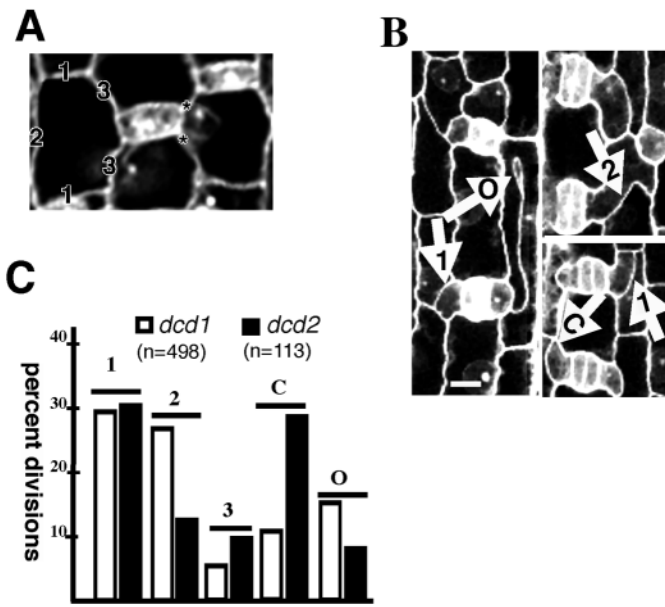


Fig. 3. Orientation of abnormal subsidiary cell divisions in *dcd1* and *dcd2*. (A) Numbers were assigned to SMC walls to classify abnormal attachment sites for subsidiary cell walls; asterisks indicate normal points of attachment. (B) Examples of the abnormal divisions observed in *dcd* mutants. The numbers in this panel correspond to the labels denoting cell wall attachment points in A and graph in C. C, corners; O, other. (C) Graph showing frequency of abnormal subsidiary walls attached at each of the SMC walls indicated in (A) in *dcd1* (white bars) and *dcd2* (black bars). Scale bar, 13 μ m.

forming divisions is $30 \pm 14\%$ ($n > 550$). We suspect that abnormal GCP divisions are not readily reflected in the final epidermal cell pattern of mutant leaves for one of two reasons. They may result in abortion of stomatal development, simply producing shorter chains of stomata in a single file and a slightly lower stomatal density. Alternatively, abnormal GMC and interstomatal cell shapes produced through these aberrant divisions may be ‘corrected’ through subsequent cell expansion to produce mature guard cells and interstomatal cells of normal shape.

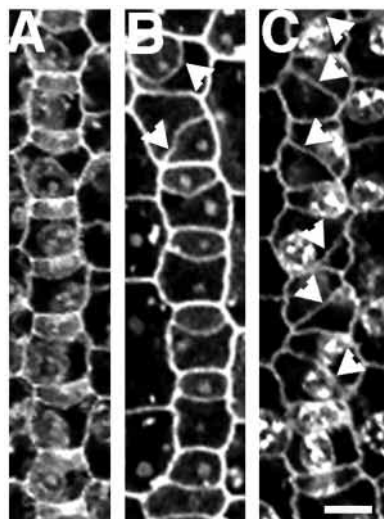


Fig. 4. Effects of *dcd* mutations on GMC formation. (A) Wild-type: a file of GMCs formed by asymmetric, transverse division of GCPs. (B) Abnormal GCP divisions (arrowheads) in *dcd1*. (C) Abnormal GCP divisions (arrowheads) in *dcd2*. Scale bar, 17 μ m.

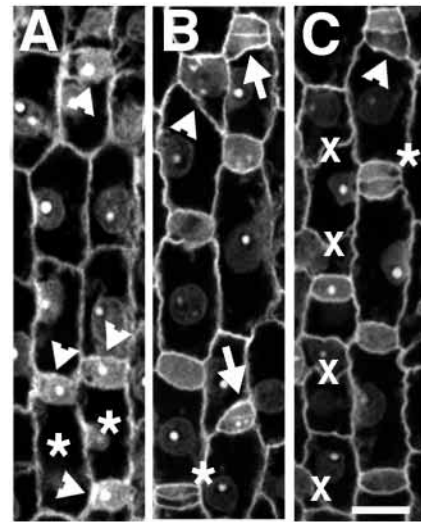


Fig. 5. Effects of *dcd* mutations on silica and cork cell formation. (A) Wild-type SCMCs (arrowheads) and two of their sister cells (indicated by asterisks) are formed by transverse, asymmetric divisions of rectangular SCPs. (B) *dcd1* epidermis with abnormally shaped SCMCs (arrowhead). In the lower left corner, a normal SCMC has divided to produce a normal silica-cork cell pair (asterisk). Two of the abnormal SCMCs have also divided (arrows). (C) *dcd2* epidermis with an abnormal SCMC that has divided (arrowhead) and several normal SCMCs, one of which has also divided (asterisk). Abnormal subsidiary cell walls from the neighboring file have been marked with an ‘x’ so that they are not confused with the silica and cork cell divisions. Scale bar, 20 μ m.

Silica and cork cell divisions

Like stomata, silica and cork cells also form by means of asymmetric divisions. In wild-type leaves, the first step in silica and cork cell formation is migration of a premitotic nucleus to the apical end of a rectangular cell referred to here as a silica-cork progenitor (SCP; Fig. 5A). This nucleus divides and a new cell wall forms around the apical daughter nucleus, forming a small, lens-shaped cell referred to here as a silica-cork mother cell (SCMC; arrowheads, Fig. 5A). Subsequently, SCMCs divide transversely to produce silica and cork cells; this division is slightly asymmetric so that the apical silica cell is somewhat smaller than the basal cork cell (asterisks in Fig. 5B,C). SCMC formation in *dcd1* and *dcd2* mutants follows the same sequence as wild-type, except that the divisions producing SCMCs are often oblique, with one end of the SCMC wall attached correctly and the other end incorrectly (Fig. 5B,C, arrows and arrowheads). Since the SCMC is often misshapen, it is difficult to determine how a normal division forming silica and cork cells should appear, and therefore the extent to which *discordia* affects this second asymmetric division (Fig. 5B,C). However, TBO-stained epidermal peels of mature mutant leaves revealed examples of silica and cork cells that are beside each other instead of one above the other. This indicates that the asymmetric division of SCMCs must be sometimes disrupted in *discordia* mutants.

Asymmetric transverse divisions that form SCMCs are very similar to those forming GMCs; our criterion for distinguishing them is that GMCs form in files of square cells (Fig. 2A) whereas SCMCs form in files of rectangular cells (Fig. 5A).

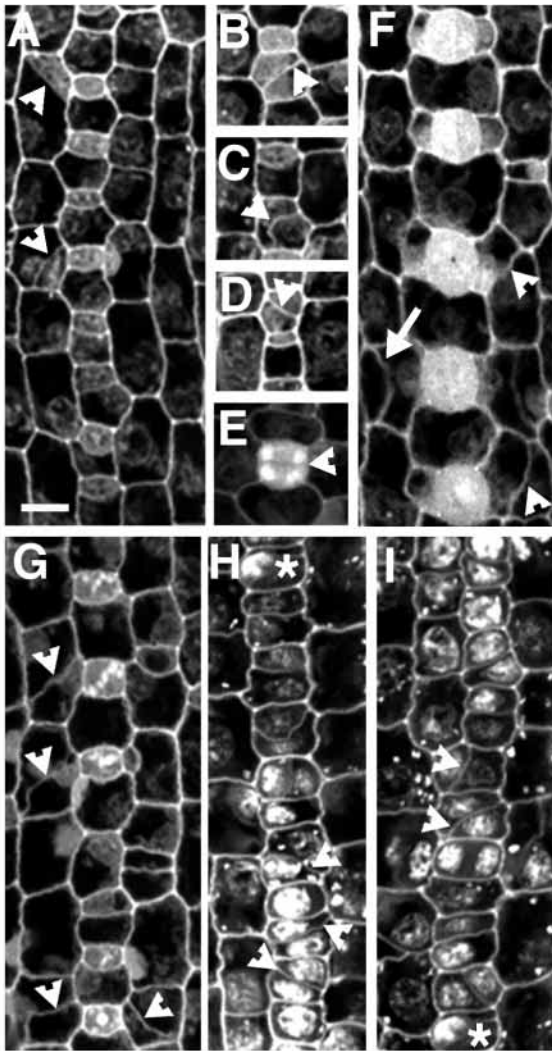


Fig. 6. Effects of cytochalasin D on wild-type and *dcd1* leaf explants. Wild-type leaf explants after exposure to 5.0 μM CD (A-E) and 10.0 μM (F) for 48 hours. (A) Arrowheads indicate the abnormally oriented subsidiary cell walls. (B-D) Abnormally oriented GMC walls (arrowheads). (E) Misoriented GC division that has occurred transversely instead of longitudinally (arrowhead). (F) After exposure to 10.0 μM CD some subsidiary walls have one end attached incorrectly (arrowheads) and some have both ends attached incorrectly (arrow). (G-I) *dcd1* leaf explants incubated on 1.0 μM CD for 48 hours. (G) Arrowheads indicate abnormally oriented subsidiary cell walls. (H,I) A stomatal file in which most of the GMCs are abnormal (asterisk indicates where the stomatal file in H continues in I). Some of the misoriented GMC walls are indicated with arrowheads. Scale bar, 17.0 μm

However, silica and cork cell pairs do occasionally form within stomatal files, so we cannot determine the frequency of abnormal SCP divisions with certainty from examination of developing leaves. However, examination of mature, TBO-stained epidermal peels showed that the frequency of abnormal silica-cork cell pairs is $19 \pm 10\%$ in *dcd1* ($n > 500$), and $40 \pm 8\%$ ($n > 300$) in *dcd2*.

In summary, both *dcd1* and *dcd2* disrupt four classes of asymmetric divisions that occur during the development of the maize epidermis: those forming GMCs, SCMCs, subsidiary

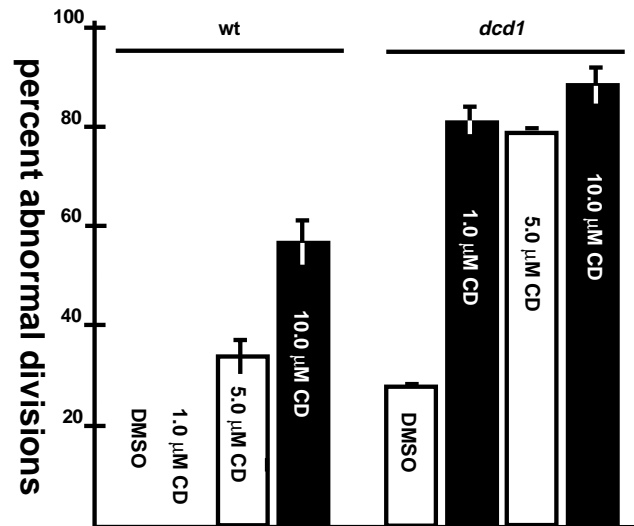


Fig. 7. Effects of CD on the frequency of abnormal subsidiary cell divisions in wild-type leaves (left half) and *dcd1* mutant leaves (right half). All treatments were done in tissue culture for 48 hours and repeated in two or more experiments. The numbers of subsidiary divisions analyzed in wild-type are: DMSO, $n > 400$; 1.0 μM CD, $n > 350$; 5.0 μM CD, $n > 750$; 10.0 μM CD, $n > 350$, and in *dcd1* are: DMSO, $n > 500$; 1.0 μM CD, $n > 600$; 5.0 μM CD, $n > 300$; 10.0 μM CD, $n > 100$. Error bars indicate standard errors.

cells, silica and cork cells. Both *discordia* mutations disrupt the proper orientation of these divisions without affecting prophase nuclear migration or nuclear division. Since the mutant leaf epidermis appears normal prior to the onset of asymmetric cell divisions (not shown), we conclude that both *discordia* mutations have no effect on the symmetric, proliferative divisions that produce most of the cells making up the leaf. Thus, the effects of these mutations are specific for asymmetric divisions.

Parallels between *discordia* phenotypes and cytochalasin effects

Previous studies have shown that cytochalasins disrupt stomatal divisions in grass leaves in a manner similar to *discordia* mutations (Cho and Wick, 1990; Pickett-Heaps et al., 1999). We tested whether the effects of *dcd* mutations on subsidiary cell divisions could be mimicked by treatment of wild-type leaf explants with cytochalasin D (CD). Wild-type leaf explants were treated in culture with either 0.5% dimethyl sulfoxide (DMSO) alone as a control, or 1.0, 5.0 or 10.0 μM CD in 0.5% DMSO for 48 hours. Like DMSO alone, 1.0 μM CD has no effect on subsidiary cell divisions. The effects of 5.0 μM CD on GMC and subsidiary cell formation are very similar to the *dcd1* phenotype: as illustrated in Fig. 6A-D, 5.0 μM CD produces subsidiary and GMC walls that are correctly attached at one end and incorrectly attached at the other. As illustrated in Fig. 7, the frequency of abnormal subsidiary cell divisions in wild-type leaf explants treated with 5.0 μM CD ($34 \pm 7\%$) is similar to that in *dcd1* mutants ($30 \pm 9\%$); GCP divisions are only occasionally misoriented. Unlike *dcd* mutations, treatment of wild-type leaf explants with 5.0 μM CD also causes misorientation of the symmetric, longitudinal division that produces the guard cell pairs (Fig. 6E). In wild-type leaves treated with 10.0 μM CD, the frequency of

abnormal subsidiary division is higher than that normally observed in *dcd1* mutants (Fig. 7). 10.0 μM CD treatment has the additional effect of misorienting both ends of the subsidiary cell wall and both ends of the GMC wall (Fig. 6F).

Since treatment of wild-type leaf explants with CD mimics the effects of *discordia* mutations on SMC and GCP divisions, mutant leaf explants were treated with CD to examine how this would affect the mutant phenotype. *dcd1* leaf explants were treated with the same concentrations of DMSO and CD that were used on wild-type. DMSO alone has no effect on cell division in *dcd1* mutants. However, treatment of *dcd1* leaf explants with 1.0 μM CD, a concentration that has no effect on wild-type, dramatically affects both SMC and GCP divisions: as illustrated in Figs 6G and 7, the frequency of abnormal subsidiary cells is increased to greater than 80%. Treatment of *dcd1* leaf explants with 1.0 μM CD does not affect the types of abnormal subsidiary cells produced: all abnormally positioned subsidiary cell walls still have one end attached correctly (Fig. 6G). In *dcd1* mutants, GCP divisions are also affected by 1.0 μM CD. As illustrated in Figs 6H and I, almost all of the GPC divisions in this stomatal file are abnormal; this was never observed in untreated *dcd1* leaves. Guard cell divisions, which are affected in wild-type leaf explants treated with 5.0 μM CD, are unaffected in *dcd1* leaf explants treated with 1.0 μM CD. Apparently, only those divisions normally affected by the *dcd1* mutation are hypersensitive to CD treatment. At 5.0 μM and 10.0 μM CD, the frequency of abnormal subsidiary divisions in *dcd1* leaves is no higher than that seen at 1.0 μM (Fig. 7). In addition, the same effects observed for wild-type leaf explants treated with 5.0 and 10.0 μM CD are also observed. Cytochalasin treatments were not performed on *dcd2* mutant leaves because even without CD treatment, the frequency of misoriented asymmetric divisions in this mutant is high and widely variable.

In summary, the *dcd1* phenotype can be mimicked by treatment of wild-type leaf explants with 5.0 μM CD. Furthermore, *dcd1* mutants are hypersensitive to the effects of CD, showing a drastic increase in the frequency of abnormal subsidiary cell and GCP divisions at a concentration five times lower than that which mimics the *dcd1* phenotype in wild-type leaves. Collectively, these data strongly suggest that *dcd1* disrupts an actin-dependent process.

Analysis of cytoskeletal arrays during subsidiary cell divisions

The effects of *discordia* mutations on asymmetric cell divisions and the results of CD experiments led us to ask how these mutations affect cytoskeletal arrays associated with establishment of division plane and formation of new walls at cytokinesis. To address this question, nuclei, microtubules and actin filaments were labeled using a whole-mount procedure in wild-type, *dcd1* and *dcd2* leaves, and visualized by confocal microscopy. Nuclei were labeled with propidium iodide, microtubules with an anti- β -tubulin antibody, and actin with FITC phalloidin.

Our observations on the cytoskeletal arrays associated with stomatal divisions in wild-type maize leaves are consistent with those described previously for other grasses and for *Tradescantia* (Cleary and Hardham, 1989; Cho and Wick, 1989, 1990; Cleary, 1995; Cleary and Mathesius, 1996). During prophase in SMCs, nuclei are in contact with the cell

cortex adjacent to the GMC and are circumscribed by PPBs of microtubules that predict the future location of subsidiary cell walls (Fig. 8A, arrowhead). In addition, a dense patch of actin is localized at the site where the nucleus contacts the cell cortex (Fig. 8D, arrowheads). Subsequently, during mitosis, a spindle is formed with one end contacting the actin patch (Fig. 8B, arrowhead). At this stage, actin filaments can be seen to radiate from the actin patch and extend approximately one quarter of the way into the spindle (Fig. 8J, arrow). Once nuclear division is complete, a phragmoplast forms between the daughter nuclei (Fig. 8A, arrow and 8E, arrowhead). These early phragmoplasts are always seen approximately 6.0 μm from the GMC wall. The phragmoplast contains both actin and microtubules and is always in contact with the inner nucleus, which itself remains in contact with the actin patch. Actin filaments are often seen extending from the nascent phragmoplast around the inner daughter nucleus to the actin patch, as well as to other cortical sites (Fig. 8E, arrow). One end of the growing phragmoplast makes contact with the cortical division site before the other. Phragmoplasts that have attached to the SMC wall at one end are usually longer and closer to the GMC than early phragmoplasts and are considered intermediate phragmoplasts. Phragmoplasts that are in contact with the longitudinal SMC wall at both ends are considered to be late phragmoplast and are on average 3.8 μm from the GMC wall (Fig. 8C, arrow and 8F, arrowhead). Thus, phragmoplasts move in toward the actin patch as cytokinesis proceeds. Unlike either early or intermediate phragmoplasts, which are often straight, late phragmoplasts are always curved and often appear to have more actin filaments connected to the actin patch.

Microtubules, actin filaments and nuclei were visualized in *dcd1* and *dcd2* and compared to wild-type. Overall, the density and organization of actin filaments and microtubules in *dcd1* and *dcd2* mutants appeared to be the same as in wild-type at each stage of the cell cycle. All of the early steps of SMC division in *dcd1* and *dcd2* are also indistinguishable from wild-type. During prophase, actin patches are present (Fig. 8J-L) and nuclei are always in contact with the actin patch in the presence of a normal PPB, indicating no defect in nuclear migration or division plane establishment (Fig. 8G, arrowheads). Spindles form with one end contacting the actin patch and with actin filaments extending from the actin patch into the spindle as in wild-type (Fig. 8H,J). Early phragmoplasts are found in the same position within the SMC as in wild-type, an average of 6.2 μm from the GMC wall (Fig. 8I, arrows). As in wild-type SMCs, actin filaments appear to connect early phragmoplasts in both *dcd1* and *dcd2* SMCs to the actin patch (Fig. 8K, arrows), as well as to other cortical sites.

Aberrant positioning of subsidiary cell walls in *dcd1* and *dcd2* mutants is apparently due to events that occur at a later stage of SMC division. Late phragmoplasts in *discordia* mutant cells are often (30% of the time in *dcd1* mutants and 50% of the time in *dcd2* mutants) farther from the GMC wall than in wild-type (Fig. 8M, arrow). Late SMC phragmoplasts in *dcd1* mutants are on average 5.0 μm from the GMC wall and 7.3 μm in *dcd2* mutants. In comparison, late phragmoplasts in wild-type are an average of 3.8 μm from the GMC wall. Late phragmoplasts in *dcd1* and *dcd2* mutants not only fail to move towards the GMC wall, but sometimes move away from it. Phragmoplasts farther than normal from the actin patch have often become dissociated from the inner daughter nucleus, but

this nucleus itself always remains in contact with the actin patch (Fig. 8N and O, arrowheads). Although phragmoplast guidance is often disrupted, one end of the late phragmoplast always attaches correctly near the GMC and actin filaments apparently connecting the phragmoplast to the actin patch are maintained (Fig. 8L, arrows).

Analysis of cytoskeletal arrays during SCP and GCP divisions

Since GCP and SCP divisions are also affected in *discordia* mutants, we examined cytoskeletal arrays in these cells giving particular attention to positioning of the phragmoplast. In both SCPs and GCPs, premitotic nuclei migrate to the apical transverse wall where a very asymmetric PPB forms (Fig. 9A and G). Following spindle formation and nuclear division, an early phragmoplast forms between the daughter nuclei (Fig. 9A, D and F). As in subsidiary cell formation, when the early phragmoplast forms in GCPs and SCPs, it is straight and at a distance from the position predicted by the PPB. In both the GCP and the SCP, the phragmoplast attaches at one end before the other; it curves tightly around the upper daughter nucleus to become attached at both ends at the position predicted by PPB (Fig. 9B, C and G). In *dcd1* and *dcd2* mutants, nuclear migration, PPB, spindle and early phragmoplast formation occurs normally in GCPs and SCPs (Fig. 9E). Nonetheless, late phragmoplasts are often mispositioned, as illustrated by the example in Fig. 9E.

Thus, in *discordia* mutants, all the early steps of asymmetric cell division in GCPs and SCPs occur normally: nuclear migration, positioning of the PPB, spindle and early phragmoplast. The consistent failure in all of these divisions is in final positioning of the phragmoplast and new cell wall to the site predicted by the PPB.

DISCUSSION

In this study, we have analyzed the effects of two non-allelic, recessive mutations with very similar phenotypes, *dcd1* and *dcd2*, on cell division during the development of the maize leaf. Both mutations disrupt four classes of asymmetric divisions occurring in the epidermis: those producing guard mother cells (GMCs) and subsidiary cells of the stomatal complex, as well as silica-cork mother cells (SCMCs), and their progeny, the silica and cork cells. The effects of these mutations appear to

be specific to asymmetric divisions, because at stages of leaf development preceding the onset of asymmetric divisions, *dcd* mutant leaves are indistinguishable from wild-type.

Fig. 10A illustrates how *dcd* mutations affect the asymmetric, transverse divisions that produce both GMCs and SCMCs. All the early steps in this process occur normally in mutant cells: actin patches, prophase nuclei, PPBs, and spindles are located normally at the apical end of the cell, and the initial position of the phragmoplast is normal as well. As cytokinesis proceeds in wild-type cells, the phragmoplast moves toward the apical end of the cell and curves tightly

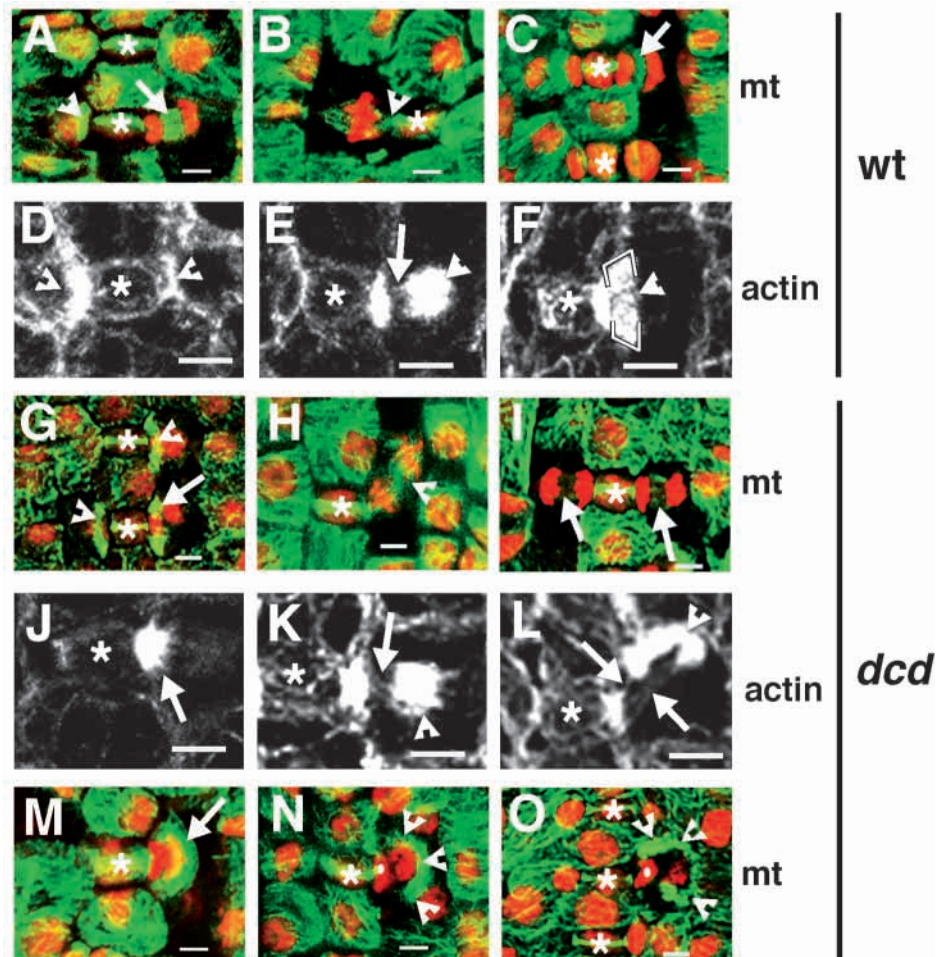


Fig. 8. The *discordia* mutations disrupt phragmoplast guidance during stomatal divisions. Asterisks indicate GMCs in all panels. Localization of microtubules by indirect immunofluorescence in wild-type (A-C) and *discordia* leaves (G-I and M-O); microtubule staining is shown in green, DNA staining in red. Actin localization is shown in wild-type (D-F) and *discordia* (J-L). (A) A PPB (arrowhead) and an early phragmoplast (arrow) are present in the SMCs flanking one of the GMCs. (B) A spindle (arrowhead) with one end oriented towards the GMC. (C) Late phragmoplast (arrow). (D) Same stage as A, arrowheads point to actin patches. (E) Arrows indicate actin filaments apparently connecting the early phragmoplast (arrowhead) to the actin patch. (F) Late actin phragmoplast (arrowhead). Black brackets demarcate the edges of the phragmoplast from the inner actin patch. (G) PPBs (arrowheads) and a normal late phragmoplast (arrow) in *dcd2*. Note that the late phragmoplast is in the same position within the SMC as the PPBs. (H) Normally oriented and attached spindle in *dcd1* (arrowheads) and (I) two early phragmoplasts of *dcd2*. (J) Same stage as H. Actin filaments radiate out from the actin patch and into the spindle (arrow). (K,L) In dividing SMCs of *dcd1*, actin filaments (arrows) extend between the actin patch and an early phragmoplast (arrowhead in K) and an aberrant late phragmoplast (arrowhead in L). (M-O) Aberrantly positioned phragmoplasts in *dcd1* (M,N) and *dcd2* (O). Note that the phragmoplasts in both (N and O) have clearly disassociated from the nucleus (white dots). Scale bar, 6.0 μm .

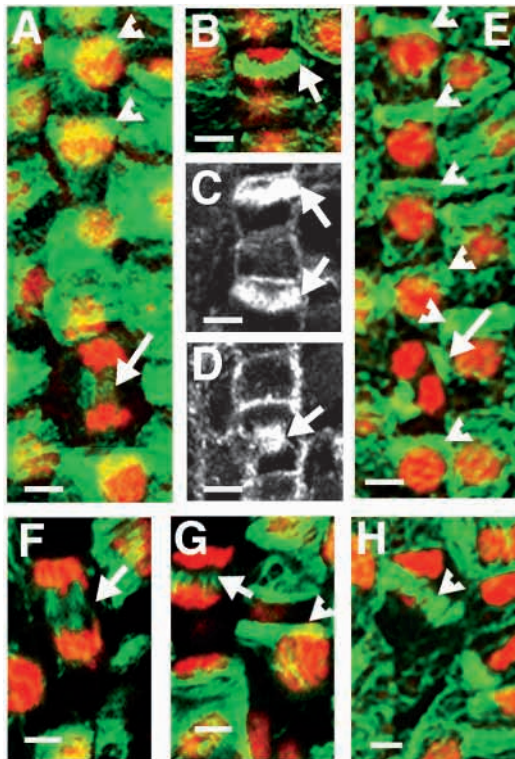


Fig. 9. Analysis of cytoskeletal arrays during GMC and SCMC formation. (A,B) Microtubules (green) and nuclei (red) of wild-type leaves: normally oriented PPBs (arrowheads) and phragmoplasts (arrows) in GCPs. The phragmoplast in A is early, whereas the phragmoplast in B is late. Note that the late phragmoplast is much closer to the position specified by the PPB than the early one. (C,D) Actin in *dcd1* mutant leaves undergoing GMC-forming divisions. Both the late phragmoplasts in C and the early phragmoplast in D are correctly positioned (arrows). (E) The late phragmoplast in a *dcd2* leaf is mispositioned (arrow); all PPBs (arrowheads) are correctly positioned. (F) An early phragmoplast in a wild-type SCP and (G) a late phragmoplast (arrows) and a PPB (arrowheads) are shown in a wild-type cell. (H) Shows an abnormally oriented SCP phragmoplast (arrowhead) in *dcd2*. Scale bar, 6.0 μm .

around the upper daughter nucleus to form a small, lens-shaped, daughter cell. In *discordia* mutants, apical movement of the phragmoplast does not always occur. The new cell wall usually attaches correctly at one end but not the other to become oblique. Sometimes the new wall is incorrectly attached at both ends so that the resulting division is nearly longitudinal.

As illustrated in Fig. 10B, the abnormalities in *dcd* subsidiary mother cell (SMC) divisions closely parallel those in GMC/SCMC-forming divisions. As in wild-type cells, SMCs appear to polarize and establish asymmetric division planes normally: nuclei migrate to positions adjacent to the GMC, and cortical actin patches and microtubule PPBs are formed in normal locations. Throughout mitosis, one end of the spindle remains in contact with the actin patch as in wild-type, and subsequently, a phragmoplast is initiated in the normal location. As cytokinesis proceeds in wild-type cells, phragmoplasts move toward the actin patch and curve tightly around the inner daughter nucleus to form a small, lens-shaped daughter cell. In contrast, phragmoplasts do not always move in toward the actin patch in mutant cells. Although the inner daughter nucleus always

remains tightly associated with the actin patch, the phragmoplast sometimes becomes dissociated from it. One end of the new cell wall usually becomes attached at the correct location, but the other end is often attached in an inappropriate position.

dcd mutants share some features in common with *tangled1* (*tan1*) mutants of maize, but are different in several respects. Both mutations cause cells to divide in abnormal orientations during maize leaf development, and both disrupt the guidance of phragmoplasts to cortical sites previously occupied by PPBs (Cleary and Smith, 1998). Compared to *dcd* mutations, which apparently affect only asymmetric, epidermal cell divisions occurring at late developmental stages, *tan1* acts much earlier in leaf development and more broadly to disrupt the proliferative divisions in all tissue layers through which most leaf cells arise (Smith et al., 1996). In *tan1* mutants, aberrantly dividing cells often have abnormal shapes and do not always orient their PPBs normally (Cleary and Smith, 1998). In contrast, aberrantly oriented divisions in *dcd* mutants occur in cells of normal shape that polarize and form asymmetric PPBs normally. Since spatial defects in phragmoplast expansion during cytokinesis are the first observable consequence of *dcd*

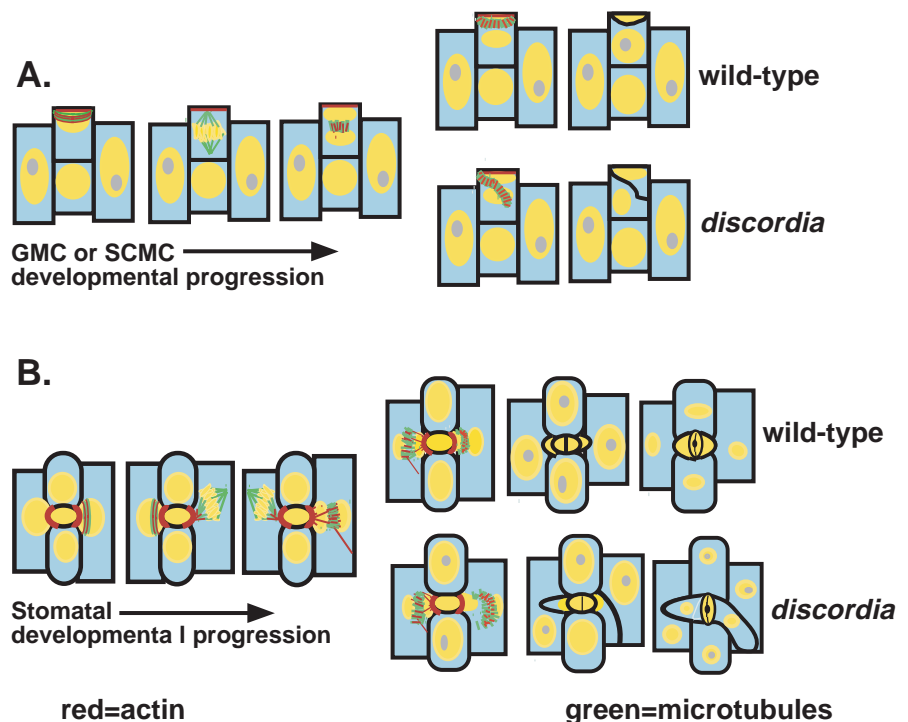


Fig. 10. Schematic summary of cytoskeletal rearrangements during asymmetric cell divisions in wild-type and *discordia* epidermal cells. (A) GMC or SCMC formation. (B) Subsidiary cell formation. Green, microtubules; red, actin.

mutations, these mutations may disrupt phragmoplast guidance in a more direct manner than *tan1*.

Cytochalasins, drugs that disrupt the actin cytoskeleton, produce effects that are more similar to *dcd* mutant phenotypes than those of any other mutation. Previous studies showed that treatment of grass leaves with cytochalasins resulted in abnormal subsidiary divisions similar to those in *dcd* mutants (Cho and Wick, 1990; Pickett-Heaps et al., 1999). Similarly, we found that treatment of wild-type maize leaves with 5 μ m CD closely mimics the effects of *dcd* mutations on subsidiary and guard cell-forming divisions. We also found that in *dcd1* mutants, these divisions are hypersensitive to CD treatment. Together, these results strongly suggest that *dcd* mutations disrupt an actin-dependent processes required for phragmoplast guidance during asymmetric cell divisions. However, CD has other effects on cell division not seen in *dcd* mutants. For example, guard cell divisions are also misoriented in wild-type leaves treated with 5 μ m CD; this was never observed in *dcd* mutants. In addition, earlier work has shown that cytochalasins can cause the spindle to become detached from the actin patch during mitosis in subsidiary mother cells (Cho and Wick, 1990; Pickett-Heaps et al., 1999). Since the phragmoplast always forms between daughter nuclei following mitosis, displacement of the spindle necessarily results in initiation of the phragmoplast in an aberrant location, possibly contributing to mislocalization of the subsidiary cell wall (Cho and Wick, 1990). In contrast, we find that the positions of spindles and early phragmoplasts are always normal in *dcd* mutant SMCs, but that phragmoplasts often fail to reach the site predicted by the PPB. Thus, the effects of *dcd* mutations are more selective than the effect of cytochalasins. Taken together, our data on *dcd* mutants suggest a role for actin in phragmoplast guidance during asymmetric cell divisions that is distinct from its role in tethering the nucleus at asymmetric, cortical sites.

In our analysis of the actin cytoskeleton, we found no changes in actin density or organization that could account for the defect in phragmoplast guidance in *dcd* mutants. In SMCs for which we gathered the greatest amount of information, we found that actin patches and cytoplasmic filaments connecting spindles and phragmoplasts to actin patches all appeared normal, even in cells dividing abnormally. One possible explanation for the misorientation of asymmetric cell divisions in *dcd* mutants is that actin filaments linking the phragmoplast to the actin patch, although present, are not effective in pulling it toward the division site. Experiments in which actin-containing cytoplasmic strands have been severed or pulled with a measurable amount of force have demonstrated that these strands are under tension (Goodbody et al., 1991; Schindler, 1995). This tension presumably depends on attachments that link cytoplasmic actin filaments to the cell cortex and nucleus, and perhaps also on motor proteins that exert a pulling force.

Interestingly, interactions between the cell cortex and nucleus mediated by tension-bearing cytoplasmic cytoskeletal filaments have been clearly shown to play a role in orienting asymmetric cell divisions during *C. elegans* embryogenesis. Prior to mitosis in certain cells of the embryo, nucleus-radiating astral microtubules attach to a specific cortical site at which several proteins are co-localized: actin and an actin-capping protein (Waddle et al., 1994), together with a component of the dynactin complex linking actin to dynein, itself a microtubule-based motor protein (Skop and White, 1998). Via this attachment, a

pulling force is exerted on the nucleus, which rotates the spindle into the proper orientation for mitosis (Hyman and White, 1987; Hyman, 1989; Skop and White, 1998). An apparently similar process occurs in zygotes of the brown algae, *Fucus* and *Pelvetia*. Prior to the first cell division, embryos become polarized and the future rhizoid pole is marked by a cortical actin patch; nucleus-radiating, astral microtubules contact the cortical actin patch and appear to mediate rotation of the nucleus into the proper orientation for the ensuing, asymmetric cell division (Allen and Kropf, 1992; Kropf, 1997). By analogy with these models, it may be that *Dcd* genes encode proteins involved in attachment of cytoplasmic actin filaments to the phragmoplast and/or actin patch, or actin-based motor proteins that apply tension to these actin filaments.

Another possible explanation for the role of *Dcd* in orienting asymmetric cell divisions comes from our observations on the association between phragmoplasts and daughter nuclei. In wild-type cells, phragmoplasts in all the classes of asymmetric divisions we examined are initially straight, and are closely associated with the daughter nuclei. As the inner nucleus condenses, the phragmoplast moves in with it and curves tightly around it to form connections with the established cortical division site. In many mutant cells where phragmoplasts were mispositioned, the phragmoplast had clearly become dissociated from the inner daughter nucleus (Fig. 8N and O, arrowheads; Figure 10). In addition, our observations on the types of abnormal attachments made by new cell walls in mutant SMCs suggest that phragmoplasts have a tendency to remain straight rather than curving into a semi-circle (Fig. 3B). Phragmoplasts isolated from dividing tobacco BY-2 cells following rupturing of the plasma membrane and repeated centrifugation of cell contents remain associated with daughter nuclei, clearly demonstrating a physical attachment between them (Asada and Shibaoka, 1994). Attachment of phragmoplasts to daughter nuclei might be particularly important for phragmoplast guidance during asymmetric cell divisions, where the daughter nucleus associated with the actin patch could serve as a scaffold for the expanding phragmoplast and also pull it in toward the actin patch as it condenses (Cleary, 1996). According to this idea, *Dcd* genes could encode proteins involved in an actin-based attachment of phragmoplasts to daughter nuclei, which assist in the proper positioning of phragmoplasts and new cell walls during asymmetric cell division.

Our data thus suggest possible roles for actin in phragmoplast guidance during asymmetric divisions that are separate from its role in establishment of cell polarity, establishment of the division site, and attachment of nuclei to the cell cortex. Elucidation of the role of *Dcd* gene products in asymmetric cell division will depend on cloning of these genes and molecular analysis of their products.

We gratefully acknowledge financial support for this work from the National Institute of Health (Grant No. R01-GM53137 to L. G. S.) and the Curriculum in Genetics and Molecular Biology at the University of North Carolina at Chapel Hill (NRSA T32 GM07092-21 and -22 for K. G.) We thank the Maize Genetics Cooperation Stock Center for seeds. Tony Perdue of the D. P. Costello Microscopy Facility (UNC-CH) and Jeffrey Price of the Quantitative Microscopy Facility (UCSD) provided valuable assistance with confocal microscopy. Susan Whitfield (of UNC-CH) provided both computer and graphics support. We thank Jen Boy and Rebecca Walker for help with mutant screens

in which these mutants were isolated. We are grateful to Punita Nagpal, Hilli Passas, Mary Frank, Anne Sylvester, Raffi Aroian and Robert Schmidt for insightful and stimulating discussion. We specially thank Ann Cleary for critical reading of the manuscript and for contributing greatly to our understanding of these mutations.

REFERENCES

- Allen, V. W. and Kropf, D. L. (1992). Nuclear rotation and lineage specification in *Pelvetia* embryos. *Development* **115**, 873-883.
- Asada, T. and Shibaoka, H. (1994). Isolation of polypeptides with microtubule-translocating activity from pramooplasts of tobacco BY-2 cells. *J. Cell Sci.* **107**, 2249-2257.
- Beckett, J. B. (1994). Locating recessive genes to chromosome arm with B-A translocations. In *The Maize Handbook*. (ed. Freeling, M. and Walbot, V.), pp. 315-327. Springer-Verlag, NY.
- Cho, S.-O. and Wick, S. M. (1989). Microtubule orientation during stomatal differentiation in grasses. *J. Cell Sci.* **92**, 581-594.
- Cho, S.-O. and Wick, S. M. (1990). Distribution and function of actin in the developing stomatal complex of winter rye (*Secale cereale* cv. Puma). *Protoplasma* **157**, 154-164.
- Cleary, A. L. (1995). F-actin redistributions at the division site in living *Tradescantia* stomatal complexes as revealed by microinjection of rhodamine-phalloidin. *Protoplasma* **185**, 152-165.
- Cleary, A. L. (1996). Regulation of cell division during formation of stomatal complexes: Importance of the actin cytoskeleton, cell plate realignments and the cell wall. In *The Symposium of the Construction of Cytoskeletal Arrays in Plant Cells*, Osaka University, Japan.
- Cleary, A. L. and Hardham, A. R. (1989). Microtubule organization during development of stomatal complexes in *Lolium rigidum*. *Protoplasma* **149**, 67-81.
- Cleary, A. L. and Mathesius, U. (1996). Rearrangement of F-actin during stomatogenesis visualized by confocal microscopy in fixed and permeabilized *Tradescantia* leaf epidermis. *Bot. Acta.* **109**, 15-24.
- Cleary, A. L. and Smith, L. G. (1998). The *Tangled1* gene is required for spatial control of cytoskeletal arrays associated with cell division during maize leaf development. *Plant Cell* **10**, 1875-1888.
- Eady, C., Lindsey, K. and Twell, D. (1995). The significance of microspore division and division symmetry for vegetative cell-specific transcription and generative cell differentiation. *Plant Cell* **7**, 65-74.
- Galatis, B., Apostolakis, P., Katsaros CHR. (1984). Experimental studies on the function of the cortical cytoplasmic zone of the preprophase microtubule band. *Protoplasma* **122**, 11-26.
- Gallagher, K. and Smith, L. G. (1997). Asymmetric cell division and cell fate in plants. *Curr. Opin. Cell Biol.* **9**, 842-848.
- Giles, K. L. and Shehata, A. I. (1984). Some observations on the relationships between cell division and cell determination in the epidermis of the developing leaf of corn (*Zea mays*). *Bot. Gaz.* **145**, 60-65.
- Goodbody, K. C., Ververloo, C. J. and Lloyd, C. W. (1991). Laser microsurgery demonstrates that cytoplasmic strands anchoring the nucleus across the vacuole of premitotic plant cells are under tension. Implications for division plane alignment. *Development* **113**, 931-939.
- Gunning, B. E. S. (1982). The cytokinetic apparatus: its development and spatial regulation. In *The Cytoskeleton in Plant Growth and Development*. (ed. C. W. Lloyd), pp. 229-292. Academic Press, London.
- Gunning, B. E. S. and Wick, S. M. (1985). Preprophase bands, phragmoplasts and spatial control of cytokinesis. *J. Cell Sci.* **2** Supplement, 157-179.
- Horvitz, H. R. and Herskowitz, I. (1992). Mechanisms of asymmetric cell division: two Bs or not two Bs that is the question. *Cell* **68**, 237-255.
- Hyman, A. A. and White, J. G. (1987). Determination of cell division axes in the early embryogenesis of *Caenorhabditis elegans*. *J. Cell Biol.* **105**, 2123-2135.
- Hyman, A. A. (1989). Centrosome movement in the early divisions of *Caenorhabditis elegans*: a cortical site determining centrosome position. *J. Cell Biol.* **109**, 1185-1193.
- Kakimoto, T. and Shibaoka, H. (1987). Actin filaments and microtubules in the preprophase band and phragmoplast of tobacco cells. *Protoplasma* **140**, 151-156.
- Kennard, J. L. and Cleary, A. L. (1997). Pre-mitotic nuclear migration in subsidiary mother cells of *Tradescantia* occurs in G1 of the cell cycle and requires F-actin. *Cell Motil. Cytoskel.* **36**, 55-67.
- Kropf, D. L. (1997). Induction of polarity in fucoid zygotes. *Plant Cell* **9**, 1011-1020.
- Liu, B. and Palevitz, B. A. (1992). Organization of cortical microfilaments in dividing root cells. *Cell Motil. Cytoskel.* **23**, 252-264.
- Lloyd, C. W. and Traas, J. A. (1988). The role of F-actin in determining the division plane of carrot suspension cells. Drug studies. *Development* **102**, 211-221.
- Minoyuki, Y. and Palevitz, B. (1990). Relationship between preprophase band organization, F-actin and the division site in *Allium*. *J. Cell Sci.* **97**, 283-295.
- Minoyuki, Y. and Gunning, B. E. S. (1990). A role for preprophase bands of microtubules in maturation of new cell walls, and a general proposal on the function of preprophase band sites in cell division in higher plants. *J. Cell Sci.* **97**, 527-537.
- Ota T. (1961). The role of cytoplasm in cytokinesis in plant cells. *Cytologia* **26**, 428-447.
- Palevitz, B. A. (1980). Comparative effects of phalloidin and cytochalasin B on motility and morphogenesis in *Allium*. *Can. J. Bot.* **58**, 773-785.
- Palevitz, B. A. (1987). Actin in the preprophase band of *Allium cepa*. *J. Cell Biol.* **104**, 1515-1519.
- Palevitz, B. A. and Hepler, P. K. (1974). The control of the plane of division during stomatal differentiation in *Allium*. II. Drug studies. *Chromosoma* **46**, 327-341.
- Pickett-Heaps, J. E. and Northcote, D. H. (1966). Cell division in the formation of the stomatal complex of the young leaves of wheat. *J. Cell Sci.* **1**, 121-128.
- Pickett-Heaps, J. E., Gunning, B. E. S., Brown, R. C., Lemmon, B. E. and Cleary, A. L. (1999). The cytoplasmic concept in dividing plant cells: cytoplasmic domains and the evolution of spatially organized cell division. *Am. J. Bot.* **86**, 153-172.
- Rappaport, R. (1986). Role of the mitotic apparatus in furrow initiation. *Ann. NY Acad. Sci.* **582**, 15-21.
- Rhyu, M. S. and Knoblich, J. A. (1995). Spindle orientation and asymmetric cell fate. *Cell* **82**, 523-526.
- Salmon, E. D. (1989). Cytokinesis in animal cells. *Curr. Opin. Cell Biol.* **1**, 541-547.
- Schindler, M. (1995). The cell optical displacement assay (CODA): measurements of cytoskeletal tension in living plant cells with a laser optical trap. *Methods Cell Biol.* **49**:69-82.
- Seagull, R., Falconer, M. and Weerdenberg, C. A. (1987). Microfilaments: dynamic arrays in higher plant cells. *J. Cell. Biol.* **104**, 995-1004.
- Sharman, B. C. (1942). Developmental anatomy of the shoot of *Zea Mays*. *Ann. Bot.* **6**, 245-282.
- Skop, A. R. and White, J. G. (1998). The dynactin complex is required for cleavage plane specification in early *Caenorhabditis elegans* embryos. *Curr. Biol.* **8**, 1110-1116.
- Smith, L. G., Hake, S. and Sylvester, A. W. (1996) The *tangled1* mutation alters cell division orientation throughout maize leaf development without altering leaf shape. *Development* **122**, 481-489.
- Staeclin, L. A. and Hepler, P. K. (1996). Cytokinesis in higher plants. *Cell* **84**, 821-824.
- Stebbins, G. L. and Shah, S. S. (1960). Developmental studies of cell differentiation in the epidermis of monocotyledons I. Cytological features of stomatal development in the Gramineae. *Dev. Biol.* **2**, 177-200.
- Sylvester, A. W., Cande, W. Z. and Freeling, M. (1990). Division and differentiation during normal and *liguleless 1* maize leaf development. *Development* **110**, 985-1000.
- Sylvester, A. W., Smith, L. and Freeling, M. (1996). Acquisition of identity in the developing leaf. *Ann. Rev. Cell Dev. Biol.* **12**, 257-304.
- Tazikawa, P. A., Sil, A., Swedlow, J. R., Herskowitz, I., and Vale, R. D. (1997). Actin-dependent localization of RNA encoding a cell fate determinant in yeast. *Nature* **389**, 90-93.
- Traas, J. A., Doonan, J. D., Rawlins, D. J., Shaw, P. J., Watts, J. and Lloyd, C. W. (1987). An actin network is present in the cytoplasm throughout the cell cycle of carrot cells and associates with the dividing nucleus. *J. Cell Biol.* **105**, 387-395.
- Twell, D., Park S. K. and Lalanne, E. (1998). Asymmetric division and cell fate determination in developing pollen. *Trends Pl. Sci.* **3**, 305-310.
- Valster, A. H. and Hepler, P. K. (1997). Caffeine inhibition of cytokinesis: effect on the phragmoplast cytoskeleton in living *Tradescantia* stamen hair cell. *Protoplasma* **196**, 155-166.
- Waddle, J. A., Cooper, J. A. and Waterston, R. H. (1994). Transient localized accumulation of actin in *Caenorhabditis elegans* blastomeres with oriented asymmetric divisions. *Development* **120**, 2317-2328.
- Wick, S. M. (1991). The preprophase band. In *The Cytoskeletal Basis of Plant Growth and Form* (ed. C. W. Lloyd), pp. 231-244. Academic Press, London.